Correlation functions for lipid membrane dynamics obtained from NMR spectroscopy

Alexander A. Nevzorov,[1] Theodore P. Trouard,[2] and Michael F. Brown[1,*]
[1]*Department of Chemistry, University of Arizona, Tucson, Arizona 85721*
[2]*Department of Radiology, University of Arizona, Tucson, Arizona 85724*
(Received 15 October 1996)

Nuclear magnetic resonance (NMR) studies of the spin relaxation of lipid membranes provide a powerful tool for investigating the dynamics of these important biological structural elements. Here spectral densities of motion for various dynamical models have been fitted to ^{2}H spin-lattice relaxation rates (R_{1Z}) measured for vesicles for 1,2-dimyristoyl-*sn*-glycero-3-phosphocholine, in the liquid-crystalline state, over a broad frequency range (2.50–95.3 MHz; total of 15 magnetic-field strengths). Moreover, the corresponding ^{13}C R_{1Z} values predicted from the models have been compared to experiment from 15.0 to 151 MHz, thereby enabling unification of the NMR relaxation data for bilayer lipids. A molecular diffusion model or alternatively a three-dimensional collective fluctuation model describes best the ^{2}H and ^{13}C R_{1Z} data. To emphasize the universality of this approach, the models have also been fitted to ^{13}C R_{1Z} data for vesicles of 1,2-dipalmitoyl-*sn*-glycero-3-phosphocholine (15.0–151 MHz; eight magnetic field strengths), and the ^{2}H R_{1Z} values for the corresponding multilamellar dispersions theoretically predicted. Correlation functions have been calculated for the lipid reorientations from the analysis of NMR relaxation data. The results suggest that slower motions are predominant in the low to mid megahertz range due to noncollective molecular motions or thermal collective excitations, whereas the bilayer interior corresponds to liquid hydrocarbon. The reorientational correlation functions derived from NMR spectroscopy are compared to recent molecular-dynamics simulations of bilayer lipids in the fluid phase. [S1063-651X(97)07803-3]

PACS number(s): 87.22.Bt, 71.45.Gm, 87.64.Hd, 76.60.−k

I. INTRODUCTION

Lipid bilayers, an essential structural element of biological membranes, represent an example of soft matter having a broad dynamic hierarchy with fast local motions and slow, noncollective, and possibly collective motions [1]. Extensive NMR experimental studies of lipid bilayers have been carried out in the past [1–9] and are amenable to further analysis and theoretical interpretation. Examples of models for the reorientational dynamics of bilayer lipids in the liquid-crystalline state include discrete jumps [10], rotational diffusion [9,11], or collective excitations treated as director fluctuations [6,12,13]. As a rule it is necessary to distinguish between fast motions, which modulate the static coupling tensor arising from the quadrupolar and dipolar nuclear spin interactions, and slow motions, which further modulate the residual coupling. Most workers agree [6,8,14,15] that the nuclear spin relaxation of liquid-crystalline bilayers in the megahertz regime predominantly manifests fluctuations in the local ordering rather than faster segmental motions of the chains; further testing of this hypothesis is needed. In addition, there is the open question of whether the relatively slow order fluctuations are due to noncollective molecular motions [6,8,9,14] or, alternatively, to collective excitations of the bilayer [6,9]. Herein the authors have tested various dynamical models in closed form for their ability to describe simultaneously the ^{2}H and ^{13}C R_{1Z} relaxation rates corresponding to the same C-H bond (segment) of the bilayer lipids. A comparison of theory with experiment suggests that order fluctuations are detectable with NMR relaxation techniques and that the local bilayer viscosity corresponds to liquid hydrocarbon. Correlation functions for these stochastic motions are calculated and compared with the results of recent molecular-dynamics (MD) simulations of lipid bilayers in the fluid state.

II. THEORETICAL MODELS FOR DYNAMICS OF LIPID BILAYERS

We discuss here diffusional models and models considering thermal excitations in membranes as a continuous medium. In developing a model aiming to describe reorientations in lipids, one has as the ultimate goal an analytical expression for the irreducible correlation functions of the various segments. For second-rank interactions these are defined as

$$G_m(\tau)=\langle[D^{(2)}_{0m}(\Omega_{PL},t+\tau)-\langle D^{(2)}_{0m}(\Omega_{PL})\rangle]^* \times[D^{(2)}_{0m}(\Omega_{PL},t)-\langle D^{(2)}_{0m}(\Omega_{PL})\rangle]\rangle, \quad (1)$$

where $m=0,\ \pm1$, or ±2 is the projection index; an axially symmetric coupling tensor is assumed. Here $\mathbf{D}^{(2)}$ indicates the second-rank Wigner rotation matrix, where the Euler angles Ω_{PL} describe the orientation of the principal axis system (PAS) associated with the C-H bond (segment) relative to the main magnetic field and contain the time dependence. By introducing closure, the rotation matrix for the overall rotation Ω_{PL} can be expanded in terms of various intermediate motional frames [6,9]; cf. Fig. 1. The corresponding spectral densities are given by Fourier transformation of Eq. (1).

*Also at Division of Physical Chemistry 1, Center for Chemistry and Chemical Engineering, Lund University, S-221 00 Lund, Sweden.

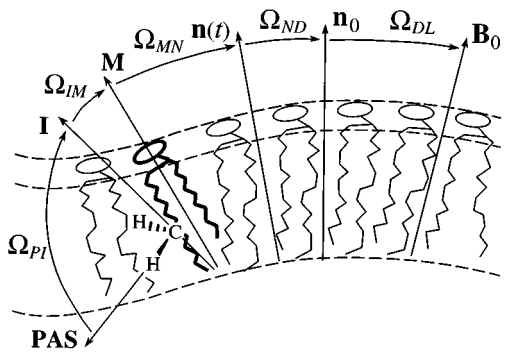

FIG. 1. Transformation of the coupling tensor, fixed to the molecule of interest, from the principal axis system (PAS) to the laboratory frame as described by the Euler angles Ω_{PL}. The various intermediate coordinate frames pertain to relaxation of the ^{2}H or ^{13}C nuclei of a lipid segment, due to electric-quadrupolar or magnetic-dipolar interactions, respectively. Euler angles Ω_{PI} transform from the PAS to an internal frame (I), Ω_{IM} to the molecular frame (M), Ω_{MN} to the instantaneous director frame [$\mathbf{n}(t)$]; Ω_{ND} to the average director or bilayer frame ($\mathbf{n}_0$), and finally Ω_{DL} to the frame of the external magnetic field ($\mathbf{B}_0$).

Let us first consider the simplest case of hindered rotational diffusion of the C-H bonds of the flexible lipid molecules in the liquid-crystalline state (model I). The lipid acyl chains comprise a system with many degrees of freedom undergoing discrete rotational isomerizations, which are treated here as a small-step diffusional process. For local segmental motions, the *static* coupling tensor in the quadrupolar or dipolar Hamiltonian is modulated by the rapid orientational fluctuations. One obtains a discrete spectrum of correlation times [6,9], which in terms of a symmetric top approximation leads to the following expression in closed form for the spectral density:

$$J(\omega)=\tfrac{1}{20}\{[1-4S^{(2)2}]j_0(\omega)+3j_2(\omega)\}. \tag{2}$$

For saturated lipid chains it can be assumed that the z axis of the segment is perpendicular to the H-C-H plane of the methylene group [6]. Note that in the case of phospholipid vesicles orientational averaging occurs, so that $J_m(\omega)\rightarrow\langle J_m(\omega)\rangle\equiv J(\omega)$, where ω is the Larmor frequency [16]. The mean-squared amplitudes are described by the second-rank order parameter $S^{(2)}\equiv\langle D^{(2)}_{00}(\Omega_{PD})\rangle$, corresponding to the segmental fluctuations with respect to the average membrane normal (director axis). For ^{2}H NMR the order parameter $S^{(2)}$ is denoted as S_{CD} and is experimentally determined from the quadrupolar splitting by $\Delta\nu_Q=\frac{3}{2}\chi_Q S_{\mathrm{CD}}$, where $\chi_Q=170$ kHz is the static quadrupolar coupling constant [15]. The reduced spectral densities $j_0(\omega)$ and $j_2(\omega)$ correspond to Lorentzians with correlation times τ_0 and τ_2, respectively. Neglecting the influence of the restoring potential, the anisotropic diffusion model gives that $1/\tau_r=[6+(\eta_D-1)r^2]D_\perp$, where τ_r are the correlation times, $\eta_D\equiv D_\parallel/D_\perp$ is the diffusion tensor anisotropy, and $r=0,2$ is the projection index.

Alternatively, one can treat the influences of slower overall motions, which are of larger angular amplitude and are superimposed on the fast segmental motions. These modulate the *residual* coupling tensor preaveraged by the local fluctuations [17]. The observed order parameter is then given by $S^{(2)}=S_f^{(2)}S_s^{(2)}$, where $S_f^{(2)}$ and $S_s^{(2)}$ are the fast and slow order parameters, and $J(\omega)=J_f(\omega)+J_s(\omega)+\text{cross terms}$ that are neglected assuming statistically independent fluctuations (e.g., time-scale separation). One possibility is to consider a restricted rotational diffusion model for the whole lipid molecule within the potential of mean torque of the bilayer (model II) [6]. Here $S_f^{(2)}=\langle D^{(2)}_{00}(\Omega_{PI})\rangle D^{(2)}_{00}(\Omega_{IM})=\langle D^{(2)}_{00}(\Omega_{PM})\rangle$, where Ω_{PI} describe the orientation of the C-H bond with respect to the intermediate frame. The flexible molecule over the longer time scale is assumed to reorient analogously to a rigid rod, having fixed values for its moments of inertia averaged over the internal degrees of freedom and thus for the principal values of the diffusion tensor **D**. One can further assume that the residual or average coupling tensor is axially symmetric with its z axis parallel to the long molecular axis. Given that $\beta_{IM}=0$ (cf. Fig. 1) leads to $J(\omega)=\frac{1}{5}S_f^{(2)2}[1-S_s^{(2)2}]j_0(\omega)$, i.e., a single Lorentzian is obtained, where $S_s^{(2)}=\langle D^{(2)}_{00}(\Omega_{MD})\rangle$. However, a single Lorentzian does not adequately describe the relaxation dispersion (not shown). Alternatively, setting $\beta_{IM}=\pi/2$ leads to

$$J(\omega)=\tfrac{1}{5}S_f^{(2)2}\{[1-S_s^{(2)2}]j_0(\omega)+3j_2(\omega)\}, \tag{3}$$

whereas intermediate values of β_{IM} yield three Lorentzians. In Eq. (3), $J(\omega)$ is scaled by the square of the fast order parameter $S_f^{(2)}$, which describes the strength of the residual coupling as a result of motional preaveraging from faster segmental motions. The full treatment of model II includes the slower molecular motions described by Eq. (3) plus the faster local segmental motions given by Eq. (2); assuming statistically independent processes, the cross terms are neglected.

The above diffusional models (I and II) represent examples of noncollective models. That is to say, a given segment or molecule is picked out of the ensemble and its diffusive motion is considered within the potential of mean torque of the bilayer. One can also explicitly treat motions of a collective nature by considering a continuous distribution of excitation modes of the bilayer director, i.e., the normal to the surface considered. Generally, the formal description of such a model can be reduced to an integral over single Lorentzians, viz., $J(\omega)=\int_{\tau_{\min}}^{\tau_{\max}}W(\tau_c)2\tau_c/[1+(\omega\tau_c)^2]d\tau_c$, where $\tau_{\max}$ and $\tau_{\min}$ are the upper and lower cutoffs for the correlation times τ_c and $W(\tau_c)$ is the distribution function of the correlation times. Let us now examine the case of collective excitations of the lipid bilayers in two or three dimensions, yielding a continuous spectrum of correlation times. For bilayer director fluctuations having small orientational amplitudes, only the Wigner elements with projection indices $m=0,\pm1$ need to be considered. The correlation function is then given, invoking the ergodic hypothesis and using Parseval's theorem, by [6,18]

$$\begin{aligned}\langle D^{(2)}_{0\pm1}(\Omega_{ND},t+\tau)^*D^{(2)}_{0\pm1}(\Omega_{ND},t)\rangle&\approx\tfrac{3}{2}\langle\delta\mathbf{n}(\mathbf{r},t+\tau)\cdot\delta\mathbf{n}(\mathbf{r},t)\rangle\\&=\frac{3}{2}\frac{1}{(2\pi)^d}\int\langle|\delta\mathbf{n}(\mathbf{q},t)|^2\rangle e^{-|\tau|/\tau_q}d^d\mathbf{q},\end{aligned} \tag{4}$$

where $\mathbf{q}$ is the wave vector and $\delta\mathbf{n}(\mathbf{r},t)$ is the vector displacement of the bilayer normal. The Fourier mean-squared amplitudes $\langle|\delta\mathbf{n}(\mathbf{q},t)|^2\rangle$ in the d-dimensional space ($d=1$, 2, or 3) and the corresponding correlation times τ_q in the single elastic constant approximation are given in terms of q^2 by applying the classical equipartition theorem [19], i.e., $\langle|\delta\mathbf{n}(\mathbf{q},t)|^2\rangle = kT/Kq^2$ and $1/\tau_q = Kq^2/\eta$, where η is the viscosity and K is the elastic constant for the bilayer deformation. Application of the equipartition theorem imposes a high-frequency limitation and enables one to deduce only the behavior of the correlation function at times $\tau \gg \hbar/kT \approx 10^{-13}$ s; this does not appear to have significant consequences within the time and frequency scales considered.

After taking the Fourier transform and calculating the integral assuming infinite upper and zero lower limits for q, the overall spectral density becomes

$$J(\omega) \propto |\langle D_{00}^{(2)}(\Omega_{PI})\rangle|^2 |\omega|^{-(2-d/2)}. \tag{5}$$

Equation (5) can be generalized to the case where the free energy is an arbitrary bilinear form of q, which can be applied to a broad range of physical systems. Thus one obtains either an $\omega^{-1/2}$ dependence ($d=3$) in the case three-dimensional (3D) director collective excitations [6,18], an ω^{-1} dependence ($d=2$) for 2D surface excitations [12,13], or an $\omega^{-3/2}$ dependence ($d=1$) for 1D undulations in polymer strings such as DNA. The resulting expressions have an effective fitting parameter B' or B [6,13] and are given by [15]

$$J(\omega) = \tfrac{1}{5} S_f^{(2)2} C' \omega^{-1} \equiv B' \omega^{-1} \quad (2\text{D fluctuations}), \tag{6a}$$

$$J(\omega) = \tfrac{1}{5} S_f^{(2)2} C \omega^{-1/2} \equiv B \omega^{-1/2} \quad (3\text{D fluctuations}), \tag{6b}$$

where C' and C include viscosity and elasticity constants of the bilayer. For the 1D and 2D cases it is necessary to introduce cutoff parameters to calculate the correlation function since the Fourier integral diverges, which makes these models somewhat more empirical. The complete treatment of models III and IV includes the contribution from faster local motions by adding Eq. (2) to Eqs. (6a) and (6b), respectively.

Let us discuss briefly the physical meaning of the models introduced above. First, one can make a general conclusion about the diffusional models applied to either segmental or molecular motions (models I and II). Despite the fact that they have been presented for heuristic purposes using simplifying assumptions (the symmetric top approximation with $\beta_{IM} = \pi/2$), the models retain the common features of any diffusional model. Namely, they give rise to a discrete spectrum of correlation times corresponding to the eigenvalues of the diffusion operator in the presence of a restoring potential. The potential is chosen so that it depends only on the Euler angle β_{PD} or β_{MD} (the potential of mean torque). Referring to Eqs. (2) and (3) and the expression for the correlation times τ_r, one can see that $j_0(\omega)$ corresponds to the stochastic rocking motion of the segment or molecule within the potential, as described by the Euler angle β_{PD} or β_{MD}, and is influenced by the order parameter $S^{(2)}$ or $S_s^{(2)}$, which describes the mean-squared amplitude. The second term $j_2(\omega)$ includes the stochastic rotation or spinning of the segment or molecule around the diffusional principal axis and corresponds to a nutation or wobbling motion. In a more general treatment [11], one obtains an infinite, yet discrete, spectrum of correlation times yielding an infinite sum of Lorentzians in the expression for the overall spectral density. By contrast, the collective fluctuation models are described by a continuous spectrum of correlation times, which arises from consideration of the thermal excitations of the bilayer director formulated in terms of wavelike disturbances. The various modes of excitations include undulations of the flexible bilayer surface (model III) and twist, splay, and bend for the hydrocarbon interior of the bilayer (model IV). It follows that the spectral density depends on an exponent of ω, which reflects the choice of the functional form of the free energy and the dimensionality of the space considered.

III. TESTING DYNAMICAL MODELS BY NUCLEAR MAGNETIC RESONANCE SPECTROSCOPY

How can one experimentally test the above formulations for the lipid bilayer dynamics? Following the classic work of Bloom *et al.* [1], the theory of NMR relaxation can be used to obtain relationships between the various observable spin relaxation rates and the spectral densities of motion corresponding to Eq. (1). Thus an applicable model should describe the relaxation data pertinent to a molecular segment regardless of the experimental technique. In terms of an irreducible representation, the fluctuations of the coupling Hamiltonian for rank-2 interactions can be written in a unified manner [4,20] as

$$\hat{H}_\lambda(t) - \langle \hat{H}_\lambda \rangle = C_\lambda \sum_m (-1)^m T_{-m}^{(2)\text{lab}} [V_m^{(2)\text{lab}}(t) - \langle V_m^{(2)\text{lab}} \rangle], \tag{7}$$

where $\lambda = D, Q$ for the magnetic-dipolar and the electric-quadrupolar coupling, respectively. Expressions for the irreducible tensor operators $T_m^{(2)\text{lab}}$ and the orientationally dependent coupling tensor $V_m^{(2)\text{lab}}$ as well as the interaction constant C_λ are given in Ref. [15]; the angular brackets indicate a time or ensemble average. The coupling tensor $V_m^{(2)\text{lab}}$ is transformed to the laboratory frame from the PAS utilizing the properties of spherical tensors under rotations, viz., by $V_m^{(2)\text{lab}} = \Sigma_s V_s^{(2)\text{PAS}} D_{sm}^{(2)}(\Omega_{PL})$.

The evolution of the density matrix ρ' in the interaction picture then yields that

$$\frac{\partial \rho'}{\partial t} = -\tfrac{1}{2} [C_\lambda V_0^{(2)\text{PAS}}]^2 \sum_{m=-2}^{2} \sum_q J_m(\omega_{m,q}) \times [T_{m,q}^{(2)\text{lab}}, [T_{-m,q}^{(2)\text{lab}}, \rho']], \tag{8}$$

where $T_{m,q}^{(2)\text{lab}}$ are the terms corresponding to the spin angular momentum operators in the $T_m^{(2)\text{lab}}$s describing the coupling [15] and $\omega_{m,q}$ are the characteristic frequencies arising from transformation of the $T_{m,q}^{(2)\text{lab}}$s to the interaction picture. The spectral densities are here defined by $J_m(\omega_{m,q}) = \int_{-\infty}^{\infty} G_m(\tau) \exp(-i\omega_{m,q}\tau) d\tau$. Therefore, the correlation functions introduced heuristically in Eq. (1) arise directly

from treatment of the evolution of the density matrix. Evaluating the double commutators in Eq. (7), one obtains for the relaxation rate of ^{2}H Zeeman order, viz, $\langle I_Z \rangle$, that [21,22]

$$R_{1Z}(^2\mathrm{H}) = \tfrac{3}{4}\pi^2 \chi_Q^2 [J_1(\omega_D) + 4J_2(2\omega_D)], \tag{9}$$

in which $\chi_Q = e^2qQ/h = 170$ kHz is the static quadrupolar coupling constant and ω_D is the deuteron Larmor frequency. Similarly, the expression for the ^{13}C Zeeman relaxation rate under conditions of proton decoupling is [21,23]

$$R_{1Z}(^{13}\mathrm{C}) = \tfrac{3}{2} N_H \chi_D^2 [\tfrac{1}{6} J_0(\omega_\mathrm{H} - \omega_\mathrm{C}) + \tfrac{1}{2} J_1(\omega_\mathrm{C}) + J_2(\omega_\mathrm{H} + \omega_\mathrm{C})]. \tag{10}$$

Here $\chi_D = \gamma_\mathrm{H}\gamma_\mathrm{C}\hbar\langle r_{\mathrm{CH}}^{-3}\rangle$ is the static dipolar coupling constant, $N_H = 2$ for methylene groups, ω_H and ω_C are Larmor frequencies of the ^{1}H and ^{13}C nuclei, and the vibrationally averaged C-H bond distance is $\langle r_{\mathrm{CH}}^{-3}\rangle^{-1/3} = 1.14$ Å [24]. For vesicles and multilamellar dispersions, the dependence of the spectral density $J_m(\omega)$ on the projection index m vanishes on account of the additional spherical averaging due to rotational and lateral diffusion as noted above [16]. Furthermore, Eq. (10) is valid only when the ^{13}C relaxation can be described by a single exponential, i.e., when the cross-correlation effects from the decoupled protons can be neglected [25]. The justification for disregarding such influences in the case of ^{13}C R_{1Z} relaxation of lipid bilayers is given below.

IV. ANALYSIS OF EXPERIMENTAL NUCLEAR MAGNETIC RELAXATION DATA

Equations (9) and (10) provide a means of testing the various dynamical models by comparing the theoretical spectral densities in closed form to the observed spin relaxation rates; cf. Fig. 1. In the present work, frequency-dependent ^{2}H and ^{13}C R_{1Z} relaxation rates for vesicles of 1,2-dimyristoyl-*sn*-glycero-3-phosphocholine (DMPC) in the liquid-crystalline state have been analyzed. A total of 15 external magnetic-field strengths ranging from 0.382 to 14.6 T have been studied, comprising a broad range [26,27]. The noncollective segmental model (I) and molecular diffusion model (II) as well as 2D and 3D collective director fluctuation models (III and IV, respectively) have been tested by fitting them to the experimentally determined ^{2}H R_{1Z} data at different frequencies, ranging from 2.50 to 95.5 MHz [26]. As a simplifying approximation, the contribution from faster segmental motions was neglected in the fits to models II–IV. Including faster local segmental motions in models II and IV does not change significantly the fits to both the ^{13}C and ^{2}H R_{1Z} data, nor are the fitting parameters appreciably affected (not shown). Theoretical fits to ^{2}H R_{1Z} rates measured at 30 °C for DMPC, labeled with ^{2}H at the C3 acyl segment, are shown in Fig. 2. Clearly, the formulations corresponding to local segmental motions (model I) [4] and 2D director fluctuations (model III) [13] fail to describe the data. The segmental diffusion model gives a nearly constant value for the relaxation rates at higher frequencies, whereas the 2D director fluctuation model does not follow the general trend at all. The molecular diffusion model (II) fits the ^{2}H R_{1Z} rates with a total of three parameters, viz., $S_f^{(2)}$, τ_0, and

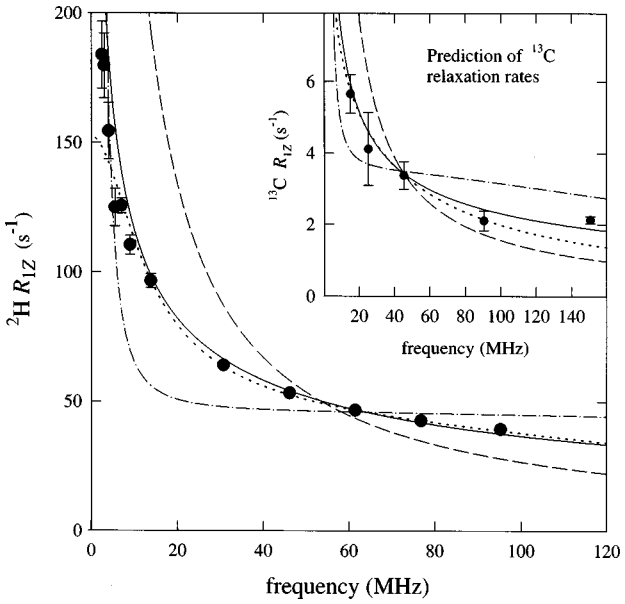

FIG. 2. Fitting of observed ^{2}H R_{1Z} relaxation rates (●) and prediction of ^{13}C R_{1Z} relaxation rates (●, inset) at 30 °C for the C3 acyl segment of DMPC vesicles in the liquid-crystalline state. Segmental diffusion (model I, ·–·–·–), molecular diffusion (model II, ·····), 2D collective fluctuations (model III, ----), and 3D collective fluctuations (model IV, ——). The small contribution from faster segmental motions has been neglected in models II–IV as a simplifying approximation. Both the molecular diffusion model ($S^{(2)} = S_{\mathrm{CD}} = 0.198$, with fitting parameters $S_s^{(2)} = 0.715$, $\tau_0 = 6.70 \times 10^{-9}$ s, and $\tau_2 = 4.60 \times 10^{-10}$ s) and the 3D director fluctuation model (fitting parameter $B = 4.48 \times 10^{-10}$ s$^{1/2}$) fit the ^{2}H R_{1Z} data and predict the ^{13}C R_{1Z} data within the experimental error, whereas the other models deviate significantly (cf. the text).

τ_2. Although the curve falls below the data at the lower frequencies, this may reflect a minor contribution from rotational tumbling of the small vesicles [14]. At higher frequencies the relaxation dispersion is not influenced by vesicle rotation ($r \geqslant 12.5$ nm) since the contribution to R_{1Z} is calculated to be only 21.0 s^{-1} at the lowest frequency (2.50 MHz) and decreases at larger values. Finally, the collective 3D director fluctuation model (IV) reproduces well the experimental values over the entire range and requires only a single effective fitting parameter B.

The next step was to test the ability of each model to describe the ^{13}C R_{1Z} relaxation rates of DMPC vesicles at natural abundance [27]. For an axially symmetric coupling tensor, the irreducible spectral densities that characterize the fluctuating ^{2}H electric-quadrupolar interaction are identical to those describing the ^{13}C-^{1}H magnetic dipolar interaction. Thus an applicable model should utilize the ^{2}H fitting results to *predict* the corresponding ^{13}C R_{1Z} rates under conditions of proton decoupling, Eq. (10); simultaneous fitting of the data is also possible. Experimentally it is observed that the ^{13}C inversion recovery curves can be fitted to within experimental accuracy by a standard three-parameter exponential function [27]. Thus it would appear that cross-correlation effects, as experimentally studied in simpler systems [28], are very difficult to quantify in the case of more complicated lipid bilayers. The expression for the ^{13}C R_{1Z} relaxation

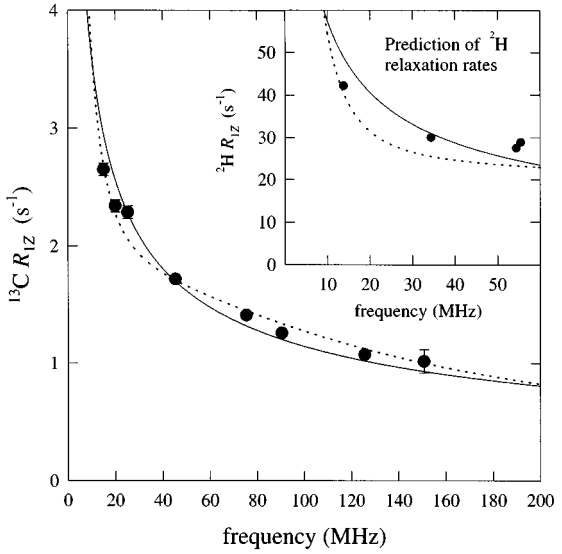

FIG. 3. Fitting of observed ^{13}C R_{1Z} relaxation rates for $(CH_2)_n$ acyl segments of DPPC vesicles (●) and prediction of ^{2}H R_{1Z} relaxation rates for C8 acyl segment of DPPC multilamellar dispersions (●, inset) at 50 °C in the liquid-crystalline state. Molecular diffusion (model II, ·····) and 3D collective fluctuations (model IV, ——); the small contribution from faster segmental motions has been neglected. The ^{2}H R_{1Z} values near 55 MHz were obtained using different NMR spectrometers [4,33] and reflect the systematic error of the measurements. Both the molecular diffusion model and the 3D collective model describe the ^{13}C and ^{2}H R_{1Z} data to within the experimental error (cf. the text).

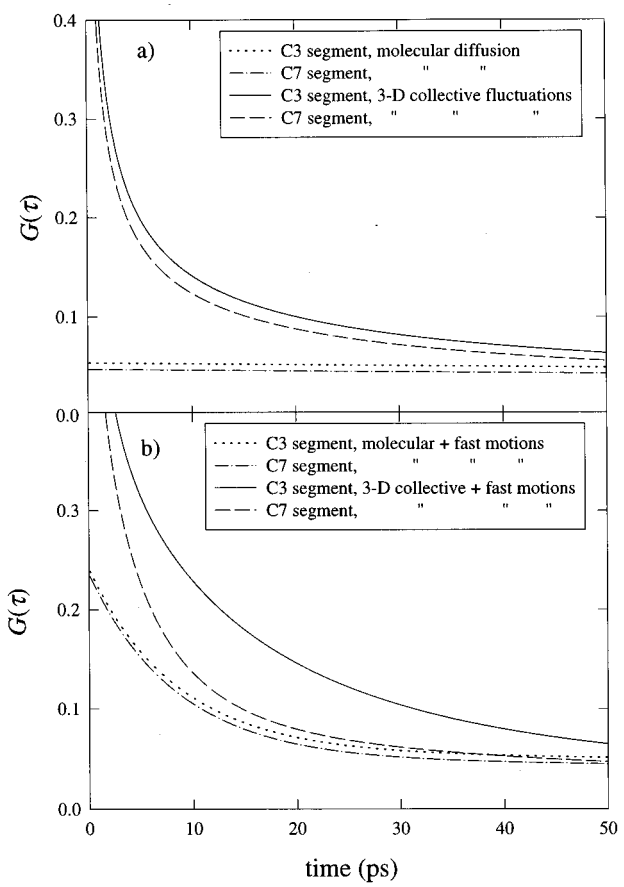

FIG. 4. (a) Second-rank correlation functions derived for orientational fluctuations of C3 and C7 acyl segments of DMPC vesicles in the liquid-crystalline state at 30 °C. Molecular diffusion (model II), C3 segment with parameters as in Fig. 2 (·····), and C7 segment with $S^{(2)}=S_{CD}=0.185$, $S_s^{(2)}=0.715$, $\tau_0=6.70\times10^{-9}$ s, and $\tau_2=4.60\times10^{-10}$ s (·–·–·–); 3D director fluctuations (model IV), C3 segment with parameters as in Fig. 2 (——), and C7 segment with $B=3.40\times10^{-10}$ $s^{1/2}$ (----). The contributions from faster segmental motions have been neglected to reveal the decay due to slow motions. Molecular rotation yields a slow decrease, whereas the 3D director fluctuations give a faster decay within the first 100 ps. (b) Effect of including faster segmental motions in the molecular diffusion model (II), with $\tau_f=8.33\times10^{-12}$ s, and in the 3D collective model (IV) with $\tau_f=1.75\times10^{-11}$ s. In this case the initial decay of the molecular diffusion correlation function over the first 50 ps is due primarily to the fast segmental motions, whereas the decrease due to molecular rotation is minimal. The correlation function for the 3D collective model is largely unaltered since the faster segmental motions overlap the time scale of the bilayer excitations (cf. the text).

rates, Eq. (10), includes spectral densities at appreciably higher frequencies, such as the term $J_2(\omega_H+\omega_C)$. For instance, if the ^{13}C resonance frequency is chosen to be 90.5 MHz, one needs to know the spectral density at up to $(\omega_H+\omega_C)/2\pi=450.2$ MHz to adequately describe the ^{13}C data at this frequency, which is due to the difference in the gyromagnetic ratios of the ^{1}H and ^{13}C nuclei. The results of the prediction of the ^{13}C R_{1Z} data from 15.0 to 151 MHz using the ^{2}H R_{1Z} fitting parameters for the C3 acyl segment of DMPC are presented in the inset to Fig. 2. Such a unified approach constitutes a rigorous test for the various proposed models since the interactions governing the ^{13}C and ^{2}H spin relaxations are described by different mechanisms and involve rather different frequency scales; cf. Eqs. (9) and (10). Again, the molecular diffusion model (II) and the 3D director fluctuation model (IV) best predict the ^{13}C data.

To emphasize the universality of the above approach vesicles of another lipid, 1,2-dipalmitoyl-*sn*-glycero-3-phosphocholine (DPPC) was studied in the fluid state. Here the reverse of the above procedure was adopted since in this case the ^{13}C R_{1Z} data are the most extensive, representing eight magnetic field strengths from 1.40 to 1.41 T. The ^{13}C R_{1Z} relaxation rates at 50 °C, measured for the $(CH_2)_n$ plateau region comprising acyl segments C4 to C13 [27], were first fitted to the molecular diffusion model (II) and 3D collective fluctuation model (IV) (*vide supra*), with the results depicted in Fig. 3. Fits to the other models, I and III, were dissatisfactory as discussed above. Then the ^{2}H relaxation data for the C8 acyl segment of the corresponding multilamellar dispersions of DPPC [16] were calculated theoretically from the ^{13}C R_{1Z} fitting parameters using Eq. (9). (In passing one should note that the ^{2}H R_{1Z} relaxation rates of DPPC vesicles and multilamellar dispersions evince few differences within experimental error [4].) A comparison of the theoretical ^{2}H R_{1Z} values to the experimental data is shown in Fig. 3 (inset); both models II and IV are similar in describing the data. It follows that the ^{13}C and ^{2}H relaxation data can be unified by assuming a predominant mechanism for the nuclear spin relaxation and then calculating the corresponding spectral densities of motion as a function of frequency.

Finally, the second-rank correlation functions $G(\tau)$, spherically averaged over all orientations, were calculated using the parameters obtained from fitting the ^{2}H relaxation to models II and IV (Fig. 4). Although both the molecular diffusion model (II) and 3D director fluctuation model (IV) describe the frequency dependence of the ^{13}C and ^{2}H relaxation rates comparably well, their Fourier transforms differ substantially when the contribution from faster local segmental motions is disregarded; cf. Fig. 4(a). For the C3 and C7 acyl chain segments of DMPC, the molecular diffusion model gives a nearly constant value of the correlation function over the first 100 ps, due to the relatively long correlation times τ_0 (rocking) and τ_2 (wobbling) obtained from the fits, on the order of 7 and 0.5 ns, respectively. The slow order parameter has a value of $S_s^{(2)}=0.715$, corresponding to restricted wobbling of the lipid molecule associated with the slow decay of the correlation function. In contrast, the correlation function for the 3D director fluctuation model yields a significant decay over the first 100 ps. The effect of including the faster local segmental motions in the above models (II and IV) is depicted in Fig. 4(b). As noted above, these motions do not greatly affect the fits of the relaxation rates as function of frequency. A comparison of Fig. 4(b) with Fig. 4(a) shows that inclusion of the faster motions alters the initial decay of the correlation function given by the molecular diffusion model (II), whereas the correlation function for the 3D collective model (IV) is similar in both cases. Due to neglect of the upper cutoffs for the wave vector of the bilayer excitation modes [cf. Eq. (4)] the continuous spectrum of correlation times for model IV effectively overlaps the time scale of the faster motions. Thus cross-correlation terms may need to be evaluated in a more detailed treatment. On the other hand, explicit consideration of finite cutoffs requires the use of an infinite series instead of the integral in Eq. (4), which makes the mathematical treatment increasingly complicated and constitutes an additional *ad hoc* assumption.

V. DISCUSSION AND CONCLUSIONS

The present research has tested various models for lipid membrane dynamics in closed form, including their ability to describe in a unified manner the frequency dispersion of both ^{13}C and ^{2}H R_{1Z} relaxation rates corresponding to the same acyl chain segment. An initial attempt has been made to obtain the reorientational correlation functions for the individual lipid segments, which involves unification of the independently obtained ^{2}H and ^{13}C NMR data. This emphasizes the importance of NMR spin relaxation techniques as a powerful tool for analyzing the dynamic properties of matter. The segmental diffusion model (I) considers a *static* coupling tensor in terms of restricted rotational isomerizations of the various C-H bonds and fails to describe adequately both ^{2}H and ^{13}C data in the low to mid megahertz range. The models involving slower motions treat the *residual* coupling tensor preaveraged by the faster segmental motions. In the molecular diffusion model (II) the lipids are assumed to reorient analogously to a rigid rod over the longer time scale, having an averaged constant diffusion tensor that represents an additional simplification. By contrast, the collective models (III and IV) consider the membrane as a continuous medium and are based on the assumption of a bilinear form of the membrane deformation energy. The two-dimensional collective fluctuation model (III) corresponds to a smectic-like picture and does not describe the ^{2}H data and predict the ^{13}C data in the megahertz range. Moreover, it is impossible to deduce an asymptotic form for the correlation function from this model since the Fourier integral of an ω^{-1} dependence diverges. The results of the present analysis show that only the molecular diffusion model (II) and the three-dimensional collective fluctuation model (IV) adequately fit the ^{2}H R_{1Z} data and predict the ^{13}C R_{1Z} data for DMPC in the liquid-crystalline state. In addition, both models II and IV fit the ^{13}C R_{1Z} data and predict theoretically the corresponding ^{2}H R_{1Z} data for another disaturated phosphatidylcholine, DPPC.

Therefore, at present both the molecular diffusion model and the 3D collective fluctuation model including the faster local segmental motions can be regarded as suitable for description of *both* the ^{2}H and ^{13}C nuclear spin relaxation rates. It follows that slower motions play a predominant role for interpretation of the observable NMR relaxation rates of lipid bilayers [2,6,15,29]. A comparison of the various models in the time domain can yield additional insights about the different physical pictures considered. Formulation of the order fluctuations in terms of a molecular diffusion model (II) gives relatively long correlation times when used to fit the experimental ^{2}H R_{1Z} relaxation rates; the initial decay of the correlation function is due primarily to the faster segmental motions. The molecular diffusion model would suggest a mean-field picture, in which the order fluctuations in lipid bilayers are due primarily to noncollective wobbling of molecules in the orienting potential. On the other hand, the 3D collective fluctuation model would emphasize explicit consideration of the entire assembly, leading to a quasinematic picture of the membrane interior for wavelengths of excitations comparable to or less than the bilayer thickness (the free-membrane limit). Physically, as mentioned elsewhere [6,30], the magnitude of the correlation times for the fast local segmental motions obtained from the fits to models II and IV, i.e., $\tau_f \approx 10^{-11}$ s, implies that the microviscosity of the bilayer interior is similar to that of a liquid hydrocarbon. However, neither model appears at present capable of fitting simultaneously the R_{1Z} frequency dependence and the orientational anisotropy of the relaxation [9,17,26], which emphasizes the need for continued experimental and theoretical investigations.

It is noteworthy that the 3D collective model (IV) together with the molecular diffusion model (II) including the faster local motions gives a decay of the correlation function consistent with recent molecular and Langevin dynamics simulations, corresponding to the individual segments of the bilayer lipids. The latter show a significant decay of the second-rank correlation functions for C-H bond fluctuations within several tens of picoseconds [30,31]. In the case of MD simulations, the force fields used to compute the dynamics of the lipid acyl segments include interactions with other parts of the molecule, as well as the mean equilibrium force field from the surrounding molecules [30–32]. More detailed models can also be considered [8,14], including as many as six fitting parameters after already a substantial reduction. Thus it seems difficult to conclude whether the good correspondence of the model to the experimental data is a conse-

quence of the correct physical picture employed or just of a larger number of fitting parameters. On the other hand, it is hard to say whether the experimentally verified $\omega^{-1/2}$ dependence indeed corresponds to collective fluctuations only or is a result of more complicated, possibly concerted, segmental motions affected by both short- and long-range interactions, analogous to those considered in the molecular-dynamics simulations. It would be more appropriate to assume, without considering specific mechanisms, that the types of motions governing the spin relaxation in lipids have a rather broad continuous spectrum of correlation times within the low to mid megahertz regime. Further refinement of this inference [6,7] can be pursued in the future with use of modern computer simulation techniques in combination with NMR relaxation measurements.

ACKNOWLEDGMENTS

This work was supported by grants from the National Science Foundation and the U.S. National Institutes of Health. We thank Yehudi Levine for helpful comments.

[1] M. Bloom, C. Morrison, E. Sternin, and J. L. Thewalt, in *Pulsed Magnetic Resonance: NMR, ESR, and Optics. A Recognition of E. L. Hahn*, edited by D. M. S. Bagguley (Clarendon, Oxford, 1992), p. 274.
[2] D. F. Bocian and S. I. Chan, Annu. Rev. Phys. Chem. **29**, 307 (1978).
[3] J. H. Davis, K. R. Jeffrey, and M. Bloom, J. Magn. Reson. **29**, 191 (1978).
[4] M. F. Brown, J. Seelig, and U. Häberlen, J. Chem. Phys. **70**, 5045 (1979).
[5] K. R. Jeffrey, T. C. Wong, E. E. Burnell, M. J. Thompson, T. P. Higgs, and N. R. Chapman, J. Magn. Reson. **36**, 151 (1979).
[6] M. F. Brown, J. Chem. Phys. **77**, 1576 (1982).
[7] M. F. Brown, A. A. Ribeiro, and G. D. Williams, Proc. Natl. Acad. Sci. U.S.A. **80**, 4325 (1983).
[8] E. Rommel, F. Noack, P. Meier, and G. Kothe, J. Phys. Chem. **92**, 2981 (1988).
[9] T. P. Trouard, T. M. Alam, and M. F. Brown, J. Chem. Phys. **101**, 5229 (1994).
[10] D. A. Torchia and A. Szabo, J. Magn. Reson. **49**, 107 (1982).
[11] P. L. Nordio and U. Segre, in *The Molecular Physics of Liquid Crystals*, edited by G. R. Luckhurst and G. W. Gray (Academic, New York, 1979), p. 411.
[12] R. Blinc, M. Luzar, M. Vilfan, and M. Burgar, J. Chem. Phys. **63**, 3445 (1975).
[13] J. A. Marqusee, M. Warner, and K. A. Dill, J. Chem. Phys. **81**, 6404 (1984).
[14] B. Halle, J. Phys. Chem. **95**, 6724 (1991).
[15] M. F. Brown and S. I. Chan, in *Encyclopedia of Nuclear Magnetic Resonance*, edited by D. M. Grant and R. K. Harris (Norell, Mays Landing, 1995), Vol. 1, p. 871.
[16] M. F. Brown and J. H. Davis, Chem. Phys. Lett. **79**, 431 (1981).
[17] M. F. Brown and O. Söderman, Chem. Phys. Lett. **167**, 158 (1990).
[18] P. Pincus, Solid State Commun. **7**, 415 (1969).
[19] P. G. de Gennes and J. Prost, *The Physics of Liquid Crystals* (Clarendon, Oxford, 1993).
[20] U. Häberlen, *High Resolution NMR in Solids. Selective Averaging* (Academic, New York, 1976).
[21] A. Abragam, *The Principles of Nuclear Magnetism* (Oxford University Press, London, 1961).
[22] R. R. Vold and R. L. Vold, Adv. Magn. Opt. Reson. **16**, 85 (1991).
[23] D. Doddrell, V. Glushko, and A. Allerhand, J. Chem. Phys. **56**, 3683 (1972).
[24] M. F. Brown, J. Chem. Phys. **80**, 2832 (1984).
[25] L. G. Werbelow and D. M. Grant, J. Chem. Phys. **63**, 4742 (1975).
[26] M. F. Brown, A. Salmon, U. Henriksson, and O. Söderman, Mol. Phys. **69**, 379 (1990).
[27] G. D. Williams, Ph. D. dissertation, University of Virginia, 1987 (unpublished).
[28] C. L. Mayne, D. M. Grant, and D. W. Alderman, J. Chem. Phys. **65**, 1684 (1976).
[29] H. M. McConnell, in *Spin Labeling. Theory and Applications*, edited by L. J. Berliner (Academic, New York, 1976), p. 525.
[30] R. M. Venable, Y. Zhang, B. J. Hardy, and R. W. Pastor, Science **262**, 223 (1993).
[31] R. W. Pastor, R. M. Venable, M. Karplus, and A. Szabo, Proc. Natl. Acad. Sci. U.S.A. **88**, 892 (1991).
[32] K. Tu, J. T. Douglas, and M. L. Klein, Biophys. J. **69**, 2558 (1995).
[33] S. W. Dodd, M.S. thesis, University of Virginia, 1987 (unpublished).